$Na_{12}K_{38}Tl_{48}Au_2$: A Metallic Zintl Phase with Naked Icosahedral Fragments Tl_7^{7-} and Tl_9^{9-} Plus Au^-

DaPing Huang, Zhen-Chao Dong, and John D. Corbett*

Ames Laboratory—DOE[1] and Department of Chemistry, Iowa State University, Ames, Iowa 50011

Received July 17, 1998

The title compound is synthesized by direct reaction of the elements at 500 °C followed by slow cooling. $Na_{12}K_{38}Tl_{48}Au_2$ crystallizes hexagonal [space group $P\bar{6}2m$ (No. 189), $Z = 1$, $a = 19.343(2)$ Å, $c = 11.498(5)$ Å] and is constituted (in terms of oxidation states) as $(Na^+)_{12}(K^+)_{38}(Tl_7^{7-})_3(Tl_9^{9-})_3(Au^-)_2$. Both clusters have C_{2v} symmetry and can be viewed as fragments of a centered icosahedral Tl_{13}. The Tl_7^{7-} cluster is an oblate pentagonal bipyramid with an apex−apex bond distance of 3.39 Å, and Tl_9^{9-} can be best derived from the centered icosahedron by removal of four adjoining vertexes (or as two fused pentagonal bipyramids). The isolated Au^- is bound in a trigonal antiprism of potassium. The compound is structurally electron-precise (Zintl phase), but it shows characteristics of a very poor metal ($\rho_{298} \sim 760\ \mu\Omega\langle$cm) with a Pauli-like susceptibility of $\sim 1.4 \times 10^{-3}$ emu·mol^{-1} over 50−300 K after correction for Larmor precession of cluster orbitals. EHMO results for the bonding in Tl_7^{7-} and factors that stabilize this compound are presented and discussed.

Introduction

Classical Zintl phases are characterized by both an electron transfer from the electropositive to the electronegative atoms (ionic part) and the formation of simple anions or anionic substructures with apparent *octet* configurations (covalent part).[2,3] Modernization of the concept to include bonding in polyanions with *delocalized* but still *closed-shell* bonding allows one to correlate structures with electron counts (e.g., via Wade's rules) in a broader range of systems. A large number of binary and ternary compounds between alkali or alkaline-earth (s-block) metals and the later main-group (p-block) elements have been characterized and almost without exception shown to meet modern Zintl criteria structurally.[3−7] The electron-poorer p elements, the triels (Tr = Al, Ga, In, Tl) in particular, are especially interesting because their compounds are expected to probe the limits of the Zintl concept and applicability.[6,8] For thallium, the array of known classic polyhedra that follow Wade's rules, the *nido*-Tl_4^{8-} (T_d) and the *closo*-Tl_5^{7-} (D_{3h})[10] and Tl_6^{8-} (O_h),[11] have been extended to include not only the classically compressed Tl_6^{6-} (D_{4h})[12] and the centered icosahedral $Tl_{13}^{10-,11-}$ (T_h, D_{3d})[13] but also two new hypoelectronic clusters Tl_9^{9-} (C_{2v})[10] and the pentacapped trigonal prismatic Tl_{11}^{7-} (D_{3h}, $2n - 4$ skeletal electrons).[14]

The variety of polyanionic species observed in alkali-metal−thallium systems gives tremendous testimony in support of the applicability of simple electron-counting rules, of the versatility possible in structures, and of the importance of suitable cavities for both the cations and the cluster anions. In particular, the increased size and packing flexibilities possible in mixed-cation systems have so far been necessary to gain certain thallium clusters, Tl_5^{7-} and Tl_9^{9-} in $Na_2K_{21}Tl_{19}$,[10] Tl_5^{7-} and Tl_3^{7-} in $Na_{23}K_9Tl_{15.3}$,[15] Tl_{13}^{10-} in $Na_4A_6Tl_{13}$ (A = K, Rb, Cs) and Tl_{13}^{11-} in $Na_3K_8Tl_{13}$,[13] and $Tl_{12}M^{12-}$ in $Na_{14}K_6Tl_{18}M$ (M = Mg, Zn−Hg).[11] (The same pertains to chains of square-planar tin in $Ca_{6.2}Mg_{3.8}Sn_7$.[16]) The present article reports the discovery of yet another thallium cluster type Tl_7^{7-} (along with a second example of Tl_9^{9-}) in the quaternary phase $Na_{12}K_{38}Tl_{48}Au_2$. A second feature is the large monatomic Au^- anions that have again[17] been found necessary to stabilize a structure with a relatively large number of alkali-metal cations per cluster (8−9). The simultaneous occurrence of three or more anionic units in a single structure is rare because of the more stringent conditions for a suitable combination of size factors and electronic requirements (closed-shell covalent bonding, Madelung energy, and consistent Fermi energy). In this case, correlations of the structure with the observed electrical and magnetic properties and Hückel MO calculations provide interesting implications regarding possible delocalization of a few high-lying electrons from highly charged anions, both of which contain thallium in an average oxidation state of −1.

(1) This research was supported by the office of the Basic Energy Sciences, Materials Sciences Division, U.S. Department of Energy. Ames Laboratory is operated for the DOE by Iowa State University under Contract No. W-7405-Eng-82.

(2) Zintl, E. *Angew. Chem.* **1939**, *52*, 1. Klemm, W.; Busmann, E. *Z. Anorg. Allg. Chem.* **1963**, *319*, 297.
(3) Schäfer, H. *Annu. Rev. Mater. Sci.* **1985**, *15*, 1.
(4) Corbett, J. D. *Chem. Rev.* **1985**, *85*, 383.
(5) Hughbanks, T. In *Inorganometallic Chemistry*; Fehlner, T., Ed.; Plenum Press: New York, 1992; p 291.
(6) Belin, C.; Tillard-Charbonnel, M. *Prog. Solid State Chem.* **1993**, *22*, 59.
(7) Kauzlarich, S., Ed. *Chemistry, Structure and Bonding of Zintl Phases and Ions*; VCH Publishers: New York, 1996.
(8) Corbett, J. D. In *Chemistry, Structure and Bonding of Zintl Phases and Ions*; Kauzlarich, S., Ed.; VCH Publishers: New York, 1996; Chapter 3.
(9) Smith, J. F.; Hansen, D. A. *Acta Crystallogr.* **1967**, *22*, 836.
(10) Dong, Z.-C.; Corbett, J. D. *J. Am. Chem Soc.* **1994**, *116*, 3429.
(11) Dong, Z.-C.; Corbett, J. D. *Angew. Chem., Int. Ed. Engl.* **1996**, *35*, 1006.
(12) Dong, Z.-C.; Corbett, J. D. *J. Am. Chem. Soc.* **1993**, *115*, 11299.
(13) Dong, Z.-C.; Corbett, J. D. *J Am. Chem Soc.* **1995**, *117*, 6447.
(14) Dong, Z.-C.; Corbett, J. D. *J. Cluster Sci.* **1995**, *6*, 187.
(15) Dong, Z.-C.; Corbett, J. D. *Inorg. Chem.* **1996**, *35*, 3107.
(16) Ganguli, A. K.; Köckerling, M.; Corbett, J. D. *J. Am. Chem. Soc.* **1998**, *120*, 1223.
(17) Dong, Z.-C.; Corbett, J. D. *Inorg. Chem.* **1995**, *34*, 5042.

10.1021/ic9808293 CCC: $15.00
Published on Web 10/08/1998

Experimental Section

Syntheses. The general techniques utilizing welded Ta tubing, glovebox operations, and Guinier powder diffraction techniques have been described elsewhere.[10] The title phase was obtained following direct reactions of Na and K (99.9%, Baker), Tl (99.998%, Johnson-Matthey), and Au (reagent grade, USDOE). All compositions were heated at 500 °C for 3 days followed by slow cooling (1 °C/h) to room temperature. Compared with the composition 12:38:48:2 for the pure compound (Na:K:Tl:Au), an exploratory composition of 24.5:24.5:49:2 gave ~70% of the title phase plus other unidentified byproducts according to the product's powder pattern. The best quality crystals of the new phase were obtained from a somewhat potassium-rich composition 9:41:48:2 with ~10% $K_{18}Tl_{20}Au_3$ and K_8Tl_{11} also present. Loading the correct stoichiometry produced a high yield of the new phase, ~96%, plus ~4% K_8Tl_{11} (the weighing accuracy was ±1 mg or ±5% for Na). An increased amount of gold did not affect the yield, while its omission caused none of the compound of interest to form. Actually, the phase can be obtained over a fairly large Na:K range (~5:45 to 30:20) as long as the Tl:Au ratio is about 48:2, although the yields naturally vary.

EDS. The elemental compositions of several single crystals were determined via energy-dispersive X-ray spectroscopy (EDS) on a JEOL 840A scanning electron microscope (SEM) with a IXRF X-ray analyzer system and a Kevex Quantum light-element detector. A beam of 20 kV and 0.3 nA was used to gain a count rate of about 2500 s^{-1}. Measurements on crystals from the first syntheses above resulted in the composition Na:K:Tl:Au = 15.6:32.8:48.3:3.3 (at. %), and for crystals from the third, 8.1:39.1:49.8:3.0.

Properties. The measurements of magnetic susceptibility were made on 99.2 mg of the purest (~96%) sample at a field of 3 T over the range of 6−300 K on a Quantum Design MPMS SQUID magnetometer. The sample was held between two fused-silica rods that were in turn fixed inside a closely fitting silica tube that was sealed at both ends under He. The raw magnetic data were corrected for the susceptibility of the container and the diamagnetism of the atom cores. Electrical resistivities of the phase were measured by the electrodeless Q method on 183 mg of the purest sample that had been sieved to a 250−425 μm powder and diluted with chromatographic Al_2O_3. Measurements were made at 34 MHz over 90−290 K.

EHMO Calculations. The EHMO program package developed by the Hoffmann group was used for bonding and charge distribution calculations. The ξ values employed (Tl: s, 2.37; p, 1.97) were taken from Kang et al.[18] while the H_{ii} values came from density functional theory (6p, −5.715 eV; 6s, −11.525 eV)[19] (see also ref 12).

X-ray Diffraction. Selection of a good crystal that gave definitive results was somewhat difficult, particularly regarding the correct hexagonal space group and the certain location of all the cations. Many crystals gave broad reflections. Film studies prior to the final data collection were found necessary in order to check the shape of the reflections as well as to establish the Laue class. The best sample was a hexagonal barlike crystal with a gray color from the second reaction above. This (sealed in a capillary) was checked by Laue, Weissenberg (*hk*0), and precession photographs (0*kl*, 1*kl*, *h*0*l*, *h*1*l*). These indicated the general equivalence of ±*h*,*k*,*l*, *h*,±*k*,*l*, *h*,*k*,±*l*, and *hkl*−*khl* reflections in a hexagonal system (a ~19.4, c ~11.4 Å), making 6/*mmm* the most probable Laue group. The crystal was mounted on a Rigaku AFC6R diffractometer equipped with a graphite monochromator and Mo Kα radiation. The least-squares refinement of 25 reflections from a random search in the range $14° < 2\theta < 18°$ yielded the hexagonal cell constants a = 19.347(6), c = 11.501(7) Å and an orientation matrix for data collection. One hemisphere of data within $3° < 2\theta < 52°$ was collected at 23 °C using $\omega-2\theta$ scans at 16°/min. Weak reflections, $I < 10\sigma(I)$, were rescanned for good counting statistics. The intensity of three standard reflections checked every 150 reflections established crystal and electronic stability during the measurements.

The data were reduced and empirically corrected for absorption on the basis of ψ-scans of six reflections, which yielded a relative transmission factor range of 0.21−1.00. The data set showed no systematic absences. There are five extinction-free space groups in the 6/*mmm* Laue class, *P*6/*mmm*, *P*$\bar{6}$2*m*, *P*$\bar{6}$*m*2, *P*622, and *P*6*mm*, but only *P*$\bar{6}$2*m* (No. 189) gave solutions of good merit from the application of direct methods with SHELXS 86[20] software. The maximal nonisomorphic subgroup *Amm*2 did not yield any reasonable solution, and solutions in other maximal nonisomorphic (and nonconforming) subgroups *P*$\bar{6}$, *P*321, and *P*31*m* were directly transformable to that in *P*$\bar{6}$2*m*. The Tl and Au atoms were directly assignable on the basis of local coordination, elemental analysis, and, eventually, electronic requirements for the overall structure (below). Subsequent refinements and Fourier mapping using the TEXSAN package[21] allowed the flagging of the K and Na atoms one by one. A residual peak of 5−6 e/Å^3 at 0, 0, 0.5 remained after the final isotropic refinement had converged at R/R_w = 5.6%/4.8%. The final anisotropic refinement resulted in R/R_w = 3.2%/2.3% with the largest residual peaks, 3.9 and −4.0 e/Å^3, at 0, 0, 0.5, 3.30 Å from K5, and at $^1/_3$, $^2/_3$, 0, respectively (both $\bar{6}$). The size of the next smaller peaks, ~±3 e/Å^3, suggested that the former were all noise. Chemically speaking, the largest residual peak, surrounded only by alkali metals, could be attributed only to an anion of Tl or Au but would at this level be crystallographically insignificant. The K5 and K7 atoms with the largest B_{iso} values refined isotropically to within 3σ of full occupancy while their B values decreased only moderately, so they were set at full occupancy.

Some details of the data collection and refinement are listed in Table 1. The atomic positions plus isotropic-equivalent displacement parameters are given in Table 2, and the closer interatomic distances are listed in Table 3. More data collection and refinement details and the

Table 1. Some Collection and Refinement Parameters for $Na_{12}K_{38}Tl_{48}Au_2$

fw	11 965.3
crystal system	hexagonal
space group, Z	*P*$\bar{6}$2*m* (No. 189), 1
lattice constants (Å)[a]	
a	19.343(2)
c	11.498(5)
volume (Å^3)	3727(3)
d_c (g/cm^3)	5.331
μ, cm^{-1} (Mo Kα)	552.46
$R(F)/R_w(F)$[b] (%)	3.1/2.3

[a] Guinier powder pattern data; λ = 1.540 562 Å; 23 °C. [b] $R = \sum||F_o| - |F_c||/\sum|F_o|$; $R_w = [\sum w(|F_o| - |F_c|)^2/\sum w(F_o)^2]^{1/2}$; $w = \sigma_F^{-2}$.

Table 2. Positional and Isotropic Displacement Parameters for $Na_{12}K_{38}Tl_{48}Au_2$[a]

atom	sym	x	y	z	B_{eq}[b]
Tl1	*m*	0.7795(1)	0.0981(1)	$^1/_2$	1.91(6)
Tl2	*mm*	0.5780(2)	0	$^1/_2$	1.7(1)
Tl3	*m*	0.6755(1)	0	0.2697(1)	1.39(9)
Tl4	1	0.67424(8)	0.16313(8)	0.3646(1)	2.64(5)
Tl5	*m*	0.1758(1)	0	0.1394(2)	2.1(1)
Tl6	*m*	0.3428(1)	0	0.2286(2)	3.0(1)
Tl7	*m*	0.8987(1)	0.2436(1)	0	2.51(8)
Tl8	*mm*	0.4402(2)	0	0	2.4(2)
Au	$\bar{6}$	$^1/_3$	$^2/_3$	0	1.27(7)
K1	*m*	0.4683(7)	0.1347(7)	$^1/_2$	2.8(4)
K2	*m*	0.2181(8)	0	$^1/_2$	2(1)
K3	*mm*	0.7882(9)	0	0	4(1)
K4	*m*	0.8706(6)	0	0.313(1)	4.1(7)
K5	$\bar{1}$	0.8218(5)	0.3343(5)	0.1585(7)	4.7(3)
K6	$\bar{6}$	$^1/_3$	$^2/_3$	$^1/_2$	3.8(6)
K7	*m*	0.6778(8)	0.1210(7)	0	4.7(6)
Na	1	0.8450(8)	0.174(1)	0.244(1)	2.8(4)

[a] Space group *P*$\bar{6}$2*m*. [b] $B_{eq} = (8\pi^2/3)\sum_i\sum_j U_{ij}a^*_i a^*_j \vec{a}_i \vec{a}_j$.

(18) Kang, D. B.; Jung, D.; Whangbo, M.-H. *Inorg. Chem.* **1990**, *29*, 257.
(19) Vela, A.; Gázquez, J.-L. *J. Phys. Chem.* **1988**, *92*, 5688.
(20) Sheldrick, G. M. *SHELXS-86*; Universität Göttingen: Göttingen, Germany, 1986.
(21) *TEXSAN*, Version 6.0; Molecular Structure Corp.: The Woodlands, TX, 1990.

Table 3. Selected Interatomic Distances (Å) in $Na_{12}K_{38}Tl_{48}Au_2$

Tl1−Tl1	3.288(4)		K1−Tl1	3.99(1)	
Tl1−Tl2	3.375(3)		K1−Tl2	4.10(1)	
Tl1−Tl3	3.292(2)	2×	K1−Tl4	3.84(1)	2×
Tl1−Tl4	3.272(3)	2×	K1−Tl4	4.05(1)	2×
Tl1−K1	3.99(1)		K1−Tl6	4.011(7)	2×
Tl1−K2	3.699(2)		K1−K5	4.017(2)	2×
Tl1−K4	3.83(1)	2×	K1−K6	3.84(1)	
Tl1−Na	3.25(1)	2×			
			K2−Tl1	3.699(2)	2×
Tl2−Tl1	3.375(3)	2×	K2−Tl6	3.94(1)	2×
Tl2−Tl3	3.251(3)	2×	K2−Na	3.98(2)	4×
Tl2−Tl4	3.158(1)	4×			
Tl2−K1	4.10(1)	2×	K3−Tl3	3.79(1)	2×
			K3−Tl7	4.086(2)	2×
Tl3−Tl1	3.292(2)	2×	K3−K4	3.94(1)	2×
Tl3−Tl2	3.251(3)		K3−K7	3.88(2)	2×
Tl3−Tl4	3.351(2)	2×	K3−Na	4.08(2)	4×
Tl3−K3	3.79(1)				
Tl3−K4	3.81(1)		K4−Tl1	3.83(1)	2×
Tl3−K7	3.872(8)	2×	K4−Tl3	3.81(1)	
Tl3−Na	3.33(1)	2×	K4−Tl5	3.647(7)	2×
			K4−K3	3.94(1)	
Tl4−Tl1	3.272(3)	2×	K4−Na	3.72(2)	2×
Tl4−Tl2	3.158(1)				
Tl4−Tl3	3.351(2)		K5−Tl4	3.907(8)	2×
Tl4−Tl4	3.114(3)		K5−Tl6	3.94(1)	
Tl4−K1	3.84(1)		K5−Tl7	3.351(9)	
Tl4−K1	4.05(1)		K5−Tl8	3.513(8)	
Tl4−K5	3.907(8)	2×	K5−Au	3.502(8)	
Tl4−K6	3.710(2)		K5−K1	4.017(2)	
Tl4−Na	3.50(2)		K5−K5	3.65(2)	
			K5−K7	4.08(1)	
Tl5−Tl5	3.207(4)		K5−Na	3.50(2)	
Tl5−Tl6	3.389(3)				
Tl5−Tl7	3.271(3)	2×	K6−Tl4	3.710(2)	6×
Tl5−K4	3.647(7)	2×	K6−K1	3.84(1)	3×
Tl5−Na	3.21(2)	2×			
			K7−Tl3	3.872(8)	2×
Tl6−Tl5	3.389(3)		K7−Tl7	3.71(1)	
Tl6−Tl7	3.267(2)	2×	K7−Tl8	3.98(1)	
Tl6−Tl8	3.233(3)		K7−K3	3.88(2)	
Tl6−K1	4.011(7)	2×	K7−K5	4.08(1)	2×
Tl6−K2	3.94(1)		K7−K7	4.05(2)	
Tl6−K5	3.463(9)	2×	K7−Na	4.01(1)	2×
Tl6−Na	3.15(1)	2×			
			Na−Tl1	3.25(1)	
Tl7−Tl5	3.271(3)	2×	Na−Tl3	3.33(1)	
Tl7−Tl6	3.267(2)	2×	Na−Tl4	3.50(2)	
Tl7−Tl7	3.394(4)		Na−Tl5	3.21(2)	
Tl7−Tl8	3.293(3)		Na−Tl6	3.15(1)	
Tl7−K3	4.086(2)		Na−Tl7	3.06(1)	
Tl7−K5	3.351(9)	2×	Na−K2	3.98(2)	
Tl7−K7	3.71(1)		Na−K3	4.08(2)	
Tl7−Na	3.06(1)	2×	Na−K4	3.72(2)	
			Na−K5	3.50(2)	
Tl8−Tl6	3.233(3)	2×	Na−K7	4.05(2)	
Tl8−Tl7	3.293(3)	2×			
Tl8−K5	3.513(8)	4×			
Tl8−K7	3.98(1)	2×			
Au−K5	3.502(8)	6×			

anisotropic displacement parameters are available in the Supporting Information, while the F_o/F_c listings and other information are available from J.D.C.

Results and Discussion

Structure. The new compound $Na_{12}K_{38}Tl_{48}Au_2$ separates evidently congruently from a sizable region in the quaternary system as long as the heavy atom ratio is approximately 25:1 or less. This remarkable phase contains Na^+ and K^+ cations together with Tl_9^{7-} and Tl_7^{7-} clusters and isolated Au^- anions in a 3:3:2 ratio, viz., as $(Na^+)_{12}(K^+)_{38}(Tl_9^{9-})_3(Tl_7^{7-})_3(Au^-)_2$ in terms of oxidation numbers. The unit cell is shown in a [001] perspective view in Figure 1. The cluster Tl_7^{7-} is centered around about 0, $^1/_4$, 0 and the equivalent, the Tl_9^{9-}, at about $^2/_3$, 0, $^1/_2$, neither a special symmetry point, whereas the gold lies on the 3-fold axes at $^1/_3$, $^2/_3$, 0 etc. Thus only the mirror planes and 2-fold axes at their junctures in $P\bar{6}2m$ are proper symmetry elements of the two clusters.

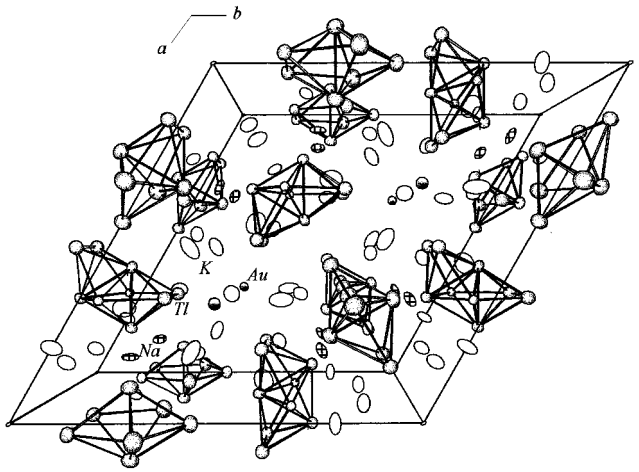

Figure 1. [001] perspective view of the cell contents of $Na_{12}K_{38}(Tl_9)_3(Tl_7)_3Au_2$ (90% probability ellipsoids). The Tl_9 and Tl_7 polyhedra (darkened) lie near $^2/_3$, 0, $^1/_2$ and 0, $^1/_4$, 0, respectively.

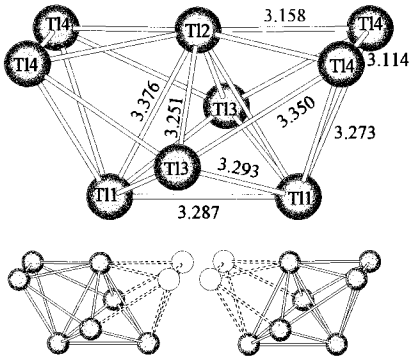

Figure 2. The Tl_9^{9-} polyhedron with independent distances. The observed cluster is C_{2v}, with mirror planes through Tl2−Tl3(×2) and Tl2−Tl1(×2).

The structure of Tl_9^{9-} illustrated in Figure 2 has C_{2v} symmetry, as does the prototype anion in $Na_2K_{21}Tl_{19}$.[10] The symmetry at Tl2 is *mm*, the two mirror planes containing pairs of Tl1 and Tl3 atoms, respectively. The Tl_9^{9-} clusters in the two compounds exhibit similar bond lengths, except that the Tl1−Tl1 and Tl4−Tl4 distances here are about 0.13 and 0.11 Å shorter than before. As discussed earlier,[10] the parentage of this hypoelectronic Tl_9^{9-} is not easily related to that of the familiar (closo) tricapped trigonal prism (D_{3h}), and the flattened face around Tl2 leaves it far from expectations for any classical deltahedron. On the other hand, the topology is close to expectations for the since-discovered centered icosahedra Tl_{13}^{11-} [13] after four adjoining vertexes are removed, which leaves the once-centering Tl2 exposed. The shorter edges around Tl2 in the open face, 3.16 Å, parallel the shorter center-to-surface average distance in Tl_{13}^{11-}, 3.24 Å, both distinctive atoms having a greater number of bonded neighbors.

The oblate anionic cluster Tl_7^{7-} shown in Figure 3 also has C_{2v} symmetry with mirror planes defined by Tl8 and two Tl7 atoms and by the pentagonal ring, the 2-fold axis passing through Tl8 and the center of the Tl5−Tl5 bond. This cluster is roughly D_{5h} in symmetry with ring distances of 3.3 ± 0.1 Å

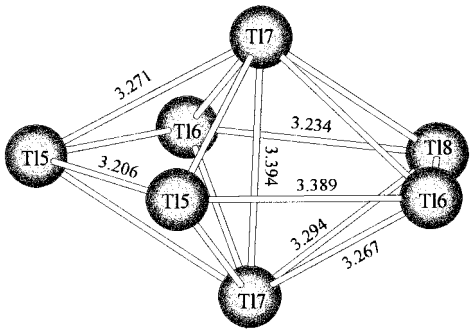

Figure 3. The Tl_7^{7-} polyhedron and bond distances. The cluster is rigorously C_{2v}, with mirror planes lying in the five-membered ring and through Tl8−Tl7(×2).

and almost equal bond angles of 108 ± 1.5° within the ring. The axial Tl7−Tl7 bond is 3.39 Å, about 0.1 Å greater than the average of other bonds but the same as the two *d*(Tl5−Tl6) within the ring. This cluster is also a fragment of the centered icosahedron, the centering atom becoming one vertex. Considering the two clusters in this compound together, one can also view Tl_9^{9-} as two fused pentagonal bipyramids, as sketched at the bottom of Figure 1. Each consists of Tl1, Tl2 (×2), Tl4 (×2) pentagonal rings with Tl2 and the other Tl1 as the vertices. The heights of the fused bipyramids in Tl_9^{9-} and that in Tl_7^{7-} are very similar, *d*(Tl1−Tl2) = 3.375(3) Å vs *d*(Tl7−Tl7) = 3.394(4) Å. Distances in the planar ring on the smaller unit average 3.29 Å, whereas ring distances in the fused units average 3.28 Å but with a fairly short *d*(Tl4−Tl4), 3.114 Å. The last may be associated with the fact that this is part of the open face of the imagined, centered isosahedral precursor. These averages are about 0.15 Å less than those in the pentagons on the surface of Tl_{13}^{11-} (D_{3d}), 3.44 Å with a range of 0.36 Å. The fact that both clusters in this compound are fragments of the known centered icosahedral Tl_{13}^{11-} is a new and useful connection. Perhaps larger pieces exist as well.

The Tl_7^{7-} cluster appears to be the first example of a naked cluster of this size without external ligands, in this case an axially compressed pentagonal bipyramid as opposed to the ideal (but unknown) *closo*-Tl_7^{9-}. The first examples of this geometry, *closo*-$B_7H_7^{2-}$ and $C_2B_5H_7$,[22−24] have not been crystallographically characterized but are not expected to have transannular bonds because of their skeletal electron counts (16). $[Au_7(PPh_3)_7]^+$ has a quite short apex−apex bond (2.58 Å, 0.28 Å less than the rest) and is therefore even more oblate,[25] but it is also heavily influenced by phosphine coordination and primary radial bonding.[26]

The isolated gold atom is surrounded by six K5 atoms at 3.50 Å, close to K−Au distances in the binary K_2Au_3, ∼3.48 Å,[27] and an average of 3.47 Å for six cations about Au^- in $K_{18}Tl_{20}Au_3$.[17] This is relevant to the existence of a similar $\bar{6}$ cavity in this compound at 0, 0, $^1/_2$ that has a 3.30 Å radius to K2 but appears to be empty (∼4.0 e/Å^3, Experimental Section) and not filled by gold. We assume that this is empty not just because of its size but mainly because of the absence of any significant quantity of excess electrons in this nominal valence compound (Zintl phase) that could be bonded by another gold atom. Iodide or bromide might also serve in the role of Au^- to stabilize (reduce repulsions within) the potassium array. As far as other cation functions, all heavy metals have contact with four to seven cations except for the less-exposed Tl2 in Tl_9^{9-}, which has only two relatively distant potassium neighbors. There are four fairly short anion−cation contacts, all with the more exposed Tl7 in Tl_7^{7-}, two each at 3.35 Å to K5 and 3.06 Å to Na plus only one other pair of cations nearby, K7 at 3.71 Å. Individually, these are not exceptionally short in comparison with shortest of these types, 3.37 and 3.11 Å, respectively, in $Na_2K_{21}Tl_{19}$,[10] the former being to the apex of Tl_5^{7-}. All cations bridge between clusters, sodium being especially effective with its six thallium neighbors at ≤3.50 Å. The slightly larger anisotropic displacements of K3, K5, and Na apparently result from the larger cavity for the first and from the asymmetric disposition of the anion neighbors for the others.

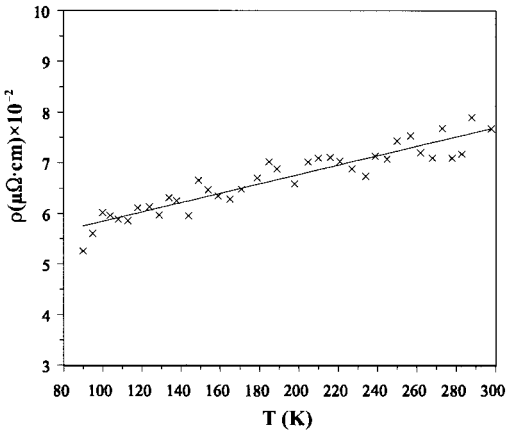

Figure 4. Molar resistivity of $Na_{12}K_{38}Tl_{48}Au_2$ ($\mu\Omega$·cm × 10^{-2}) as a function of temperature (K).

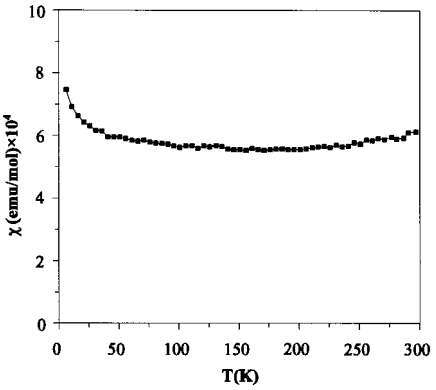

Figure 5. Molar magnetic susceptibility of $Na_{12}K_{38}Tl_{48}Au_2$ at 3 T as a function of *T* (K), corrected for core terms.

Properties. The result of electrical resistivity measurements is shown in Figure 4. The compound is a poor metallic conductor with $\rho_{298} \sim 765 \mu\Omega\langle$cm and $\partial\rho/\rho\partial T$ of ∼0.12% K^{-1}. The presence of ∼4% of impurity K_8Tl_{11} may have lowered the result slightly from the true value since $\rho_{298} \sim 230\ \mu\Omega\langle$cm and $\partial\rho/\rho\partial T$ is 0.18(1)% K^{-1} for the latter.[14] The molar magnetic susceptibilities in Figure 5 are $\sim 6.0 \times 10^{-4}$ emu·mol^{-1} over 25−300 K vs 3.6×10^{-4} emu·mol^{-1} known for the small amount of impurity K_8Tl_{11}, which would be of little effect. Note that the usual correction for the diamagnetic Larmor precession of electron pairs[28] in the large orbitals in the six clusters per mole would raise χ_p by $\sim 8.1 \times 10^{-4}$ emu·mol. The result is

(22) Aihara, J. *J. Am. Chem. Soc.* **1978**, *100*, 3339.
(23) Dewar, M. J. S.; Mckee, M. L. *Inorg. Chem.* **1978**, *17*, 1569.
(24) Siwapinyoyos, G.; Onak, T. *J. Am. Chem. Soc.* **1980**, *102*, 420.
(25) van der Velden, J. W. A.; Beurskens, P. T.; Bour, J. J.; Bosman, W. P.; Noordik, J. H.; Kolenbrander, M.; Buskes, J. A. K. M. *Inorg. Chem.* **1984**, *23*, 146.
(26) Mingos, D. M. P.; Wales, D. J. *Introduction to Cluster Chemistry*; Prentice Hall: New York, 1990; Chapter 4, p 191.
(27) Zachwieja, U. *J. Alloys Compd.* **1994**, *206*, 277.
(28) Sevov, S. C.; Corbett, J. D. *Inorg. Chem.* **1992**, *31*, 1895.

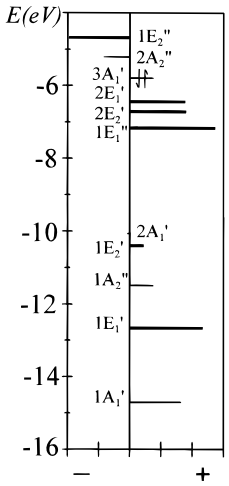

Figure 6. EHMO results for Tl_7^{7-} (D_{5h}), with $3A_1'$ as the HOMO. Heavier lines represent degenerate orbitals. Total overlap populations for each orbital are indicated on the abscissa.

still typical for a Pauli paramagnetism in this sort of compound,[8] particularly when note is made of the large formula weight ($\chi_g \sim 1.2 \times 10^{-7}$ emu·g^{-1}).

Bonding. The MO scheme, the bonding, and the relationship of Tl_9^{9-} to other polyhedra, particularly the centered icosahedral Tl_{13}^{11-} and, less directly, a D_{3h} Bi_9^{5+}-like model, were considered before.[10] Of course, the oblate Tl_7^{7-} can be readily related to the classical *closo*-Tl_7^{9-} (vice $B_7H_7^{2-}$) by axial compression. As described in more detail for the strongly compressed $Tl_9Au_2^{9-}$ (D_{3h}),[17] the distortion of Tl_7^{9-} affects particularly the symmetric (a_1') and antisymmetric (a_2'') combinations of p_z (plus s) orbitals on the axial (and waist) atoms, the former becoming the σ bond and the latter being emptied and driven higher in energy. The more quantitative calculations made for the present Tl_7^{7-} took advantage of earlier experiences regarding good choices for rather uncertain orbital parameters for thallium.[12] The EHMO results were obtained for the idealized D_{5h} model, with distances the average of those observed for the C_{2v} Tl_7^{7-}. The results are plotted in terms of both energy and total overlap population for each orbital in Figure 6, the seven plus seven ($2n$) groups of orbitals being largely s and p in character, respectively. The gap found from this particular calculation is 0.57 eV, but the energy distribution was observed to be quite sensitive to particularly the orbital size parameters. Perhaps the most credible feature is the distinctive change from bonding to antibonding overlap populations at the HOMO−LUMO gap, Figure 6. Of course, the location of E_F and the stability of the real solid depend on a lot more, particularly three-dimensional band dispersions, the appreciable Madelung energy of this compound, and, presumably, modest covalencies in cation−cluster interactions. The sizes and energies of the gaps calculated for Tl_7^{7-} and Tl_9^{9-} are quite similar at this level of approximation.

In general characteristics, the E_2 orbitals are all associated with bonding orbitals that span only the ring interactions while all E_1 and A types include ring-apex interactions. The π orbital sets in the ring in $1A_2''$, $2A_1'$, and $1E_1''$ are lowered considerably when the apex atoms are added.

The question of the relative strength of the transannular Tl7−Tl7 bond at 3.39 Å vs averages of 3.28−3.29 Å in the ring or over the surface bonds in the cluster is complex. The acute bond angles at Tl7 certainly reduce the bonding effectiveness, while contributions to the Tl7−Tl7 overlap population (OP) are diverse. Those from the lower levels are small, 0.06 for $1A_1'$, −0.060 for $1A_2'$, −0.113 for $1E_1''$, and 0.041 for $2A_1'$. Only the 0.266 OP value for $3A_1'$ (which is mainly s on the ring and p_z on the apexes) is responsible for a positive sum, 0.229. This number compares with 0.365 and 0.442 OP's for each Tl7-ring and the ring edge bond, respectively. These simple calculations give fairly uniform charges (Mulliken populations) on the atoms in the observed isolated cluster, −0.88 e$^-$ on Tl8 to −1.0 e$^-$ on Tl6. This is quite different in Tl_9^{9-}, where the charge on the unique Tl2 is about −0.44 e$^-$ vs −1.04 to −1.14 e$^-$ for the rest, and in the uncompressed $B_7H_7^{2-}$, where the apical boron atoms are said to bear charges of +0.29 e$^-$ vs −0.31 e$^-$ in the waist.[26]

The Tl7 vertexes in Tl_7^{7-} are also noteworthy in the closer approach of cations to these points, namely for four of the six K and Na neighbors, although the individual distances are not significantly different from minima found in other thallium cluster structures. One simple explanation is that the Tl7 radius is not very spherical in this unusual bonding environment. Of course, in a localized sense one could speculate that the rather small metallic conductivity observed ($\sim 1.3 \times 10^3$ Ω^{-1}·cm^{-1}) could originate with a band containing this HOMO (or that for Tl_9^{9-}) and that orbital depopulation or electron screening could affect the radius. However, this is very speculative as the conduction effect is quite small and we know nothing of the band structure of this rather complex solid. Moreover, the Tl7−Tl7 bond observed argues strongly for localization in the HOMO since this MO alone is virtually the only source of bonding (overlap population) between these atoms. As is general for this sort of compound, the behavior of a few of the highest energy electrons with regard to a conduction property does not significantly influence or define the more tightly bound electrons, the effects of which are reflected in covalent bonding effects within the clusters.[8]

Once again, we are surprised at the subtlety, complexity, and novelty that appear to enter into the existence of this phase, $(Na^+)_{12}(K^+)_{38}(Tl_7^{7-})_3(Tl_9^{9-})_3(Au^-)_2$ in an idealistic description. The needs for and advantages of mixed cations are familiar in how they "solvate" anions well, fill space in diverse arrangements better, and therewith allow the capture of new cluster species in different structures. Clusters are well-known to persist in alkali-metal−thallium melts, although which one or several are present is difficult to say.[29] Characteristics of different but unforeseen solid state structures can obviously function as very select "sieves" to sort out the different complex species. New lessons also appear. The two Au^- ions in the present phase play an essential role in capturing two excess electrons, but not a possible third even though such a cavity exists. These anions also play some significant role in stabilizing the surrounding cation atmosphere, as the compound does not form without the gold component. (Other anion formers might so serve, however.) And these and certainly other factors all come together to furnish another example of a valence (closed-shell) compound. Release of these two electrons in the absence of gold would probably populate the A_2'' MO on Tl_7^{7-}, which is strongly σ^* in the axial compression, and produce the unknown and perhaps less well bound *closo*-Tl_7^{9-}. Naturally, there would be a change in Madelung energy too, which we have not considered, and probably a change in packing and structure would be needed too, which we are totally unequipped to forecast. Nonetheless, the Tl_7^{9-} ion may still be discovered some day in other systems,

(29) van der Lugt, W. In *Chemistry, Structure and Bonding of Zintl Phases and Ions*; Kauzlarich, S., Ed.; VCH Publishers: New York, 1996; Chapter 4.

as has occurred in parallel for both Tl_6^{6-} ($\sim D_{4h}$) and Tl_6^{8-} (O_h) clusters in different compounds.[12,30]

Acknowledgment. The authors are indebted to W. Straszheim for EDS measurements, to J. Ostenson for magnetic susceptibity data, and to G. J. Miller for comments on bonding problems.

(30) Dong, Z.-C.; Corbett, J. D. *Angew. Chem., Int. Ed. Engl.* **1996**, *35*, 1006.

Supporting Information Available: Tables of additional data collection and refinement information and the anisotropic displacement parameters (2 pages). Ordering information is given on any current masthead page.

IC9808293